Cardiac Sarcoidosis: Case Report, Workup, and Review of the Literature

Cardiol Ther (2013) 2:181–197
DOI 10.1007/s40119-013-0017-0

CASE REPORT

Cardiac Sarcoidosis: Case Report, Workup, and Review of the Literature

Anna Plitt · Sharmila Dorbala ·
Michelle A. Albert · Robert P. Giugliano

To view enhanced content go to www.cardiologytherapy-open.com
Received: March 27, 2013 / Published online: June 18, 2013

ABSTRACT

Introduction: Cardiovascular disease is the leading cause of death worldwide, with coronary heart disease being the most common manifestation. While deaths attributed to coronary heart disease are falling in the developed world, the number of patients with cardiomyopathy continues to increase. In this paper, the current literature on imaging modalities for infiltrative and inflammatory cardiomyopathies is reviewed, focusing on the three most common diagnoses, namely sarcoidosis, amyloidosis, and myocarditis.

Case report: A 43-year-old male presented with palpitations and left ventricular systolic dysfunction for a second opinion following an initial nondiagnostic workup. The employed clinical and radiologic approach that led to a definitive diagnosis and disease-specific treatment is presented here.

Conclusion: The current algorithms and the strengths and weaknesses of the various radiologic techniques in establishing a diagnosis in patients who present with new onset cardiomyopathy are reviewed. Recommendations are provided regarding the selection between echocardiography, computed tomography radionuclide imaging, and magnetic resonance imaging in diagnosing the various causes of cardiomyopathy.

Keywords: Amyloidosis; Cardiomyopathy; Computed tomography; Echocardiography; Magnetic resonance imaging; Myocarditis; Radionuclide imaging; Sarcoidosis

A. Plitt
Harvard Medical School, Boston, MA, USA

S. Dorbala · R. P. Giugliano (✉)
Division of Cardiovascular Medicine, Brigham and Women's Hospital, Harvard Medical School, Boston, MA, USA
e-mail: rgiugliano@partners.org

M. A. Albert
Howard University College of Medicine, Washington, DC, USA

Enhanced content for this article is available on the journal web site: www.cardiologytherapy-open.com

INTRODUCTION

Cardiovascular disease is the leading cause of death worldwide [1]. From 1990 to 2010, the

prevalence of cardiovascular circulatory diseases has risen by 31% contributing to over 15,616,000 deaths worldwide in the year 2010 [2]. Specifically with the prevalence of cardiomyopathies rising by 40%, early diagnosis is critical in directing treatment and following progression of the disease [2, 3]. Given nonspecific symptoms and baseline tests, noninvasive imaging with echocardiography, cardiac magnetic resonance imaging (CMRI) and positron emission tomography (PET)-computed tomography (CT) performed with fluorine-18-fluoro-deoxy-glucose (FDG-PET-CT) is instrumental [1]. This report describes a case of cardiac sarcoidosis focusing on workup that led to the diagnosis. It also gives an overview of three of the most common cardiomyopathies: amyloidosis, myocarditis, and sarcoidosis and their workup with various imaging modalities namely echocardiography, CMRI, and FDG-PET.

The analysis in this article is based on previously conducted studies, and does not involve any new studies with human or animal subjects performed by any of the authors.

CASE REPORT

A 43-year-old Caucasian man with history of premature ventricular contractions (PVCs) and mild-moderate left ventricular (LV) systolic dysfunction with normal LV dimensions on echocardiogram performed at an outside institution was admitted from the clinic after a second opinion with a chief complaint of increasing palpitations over a period of 2 months. The patient did not smoke, denied chest discomfort, shortness of breath with daily activities, paroxysmal nocturnal dyspnea, and orthopnea. There was no history of hypertension, dyslipidemia, coronary artery disease (CAD), and no family history of premature CAD or stroke. The patient also did not have a recent history of severe illness, respiratory or otherwise, or travel outside of the United States.

On physical examination, the patient appeared physically fit in no apparent distress. The vital signs were temperature 97.8 F, blood pressure 137/71 mmHg, heart rate 45 beats/min (bpm), respiratory rate 18 breathes/minute, and oxygen saturation 100% on room air. There was no jugular venous distention and no carotid bruits. Lungs were clear to auscultation. Palpation of the heart was unremarkable. The heart rate was regular with an occasional premature beat. The first and second heart sounds were normal, and no murmurs, rubs, or gallops were appreciated. The abdomen was soft, nontender, nondistended, with no hepatosplenomegaly. There was no peripheral clubbing, cyanosis, or edema. No skin lesions were noted.

Laboratories were notable only for hyperlipidemia (Table 1); cardiac troponin T, creatine kinase (CK), CK-myocardial band, and brain natriuretic peptide were all within normal limits. The 12-lead electrocardiogram (ECG) demonstrated a junctional rhythm with frequent PVCs and a right bundle branch morphology (Fig. 1). Repeat echocardiography was notable for mild-moderate dilation of the left ventricle, with overall mild-moderate reduction of LV systolic function with an ejection fraction (EF) of 40%. The basal-to-mid inferoposterior wall was akinetic, and the inferior wall and apex were severely hypokinetic. The LV wall thickness was normal and the right ventricular (RV) size and function, atria, pericardium, and pleura were each normal. A standard Bruce Protocol exercise stress test was carried out to assess for potential underlying etiology that led to the patient's

Table 1 Admission laboratory values

	Results	Reference range
Cardiac tests		
Brain natriuretic peptide	37	0–100 (pg/mL)
Creatine kinase	129, 91, 118	41–266 (U/L)
Creatine kinase-myocardial band	0.7, 0.7, 2.0	0.0–6.6 (ng/mL)
Myoglobin	24.08	0–100 (ng/mL)
Troponin	<0.04 (×3)	0.00–0.04 (ng/mL)
Complete blood count		
White blood cells	5.18	4–10 (K/μL)
Hematocrit	39.1	40–54 (%)
Platelets	222	150–450 (K/μL)
Lipid test		
Cholesterol	235	140–199 (mg/dL)
Triglycerides	145	35–150 (mg/dL)
HDL cholesterol	57	40–100 (mg/dL)
LDL cholesterol calculated	149	50–129 (mg/dL)
Chemistry		
Sodium	138	136–145 (mmol/L)
Potassium	3.7	3.4–5.0 (mmol/L)
Chloride	107	98–107 (mmol/L)
Carbon dioxide	22	22–31 (mmol/L)
Blood urea nitrogen	18	6–23 (mg/dL)
Creatinine	0.94	0.50–1.20 (mg/dL)
Glomerular filtration rate	88	NA
Glucose	94	70–100 (mg/dL)
Liver function tests		
Alanine aminotransferase	16	10–50 (U/L)
Aspartate aminotransferase	15	10–50 (U/L)
Alkaline phosphatase	47	35–130 (U/L)
Bilirubin	0.6	0.0–1.0 (mg/dL)
Infectious		
Lyme antibody	Negative	Negative
Human Immunodeficiency Virus-Antibody	Nonreactive	Nonreactive
Immunology		
C-reactive protein	0.8	0.0–3.0 (mg/dL)
Erythrocyte sedimentation rate	4	0–12 (mm/h)

HDL High density lipoprotein, *LDL* low density lipoprotein

ECG findings with exercise [4]. The patient exercised for 15 min and 15 s, achieving a maximum heart rate of 160 bpm (90% of the maximum predicted for the patient's age) and blood pressure of 166/70 mmHg. No ischemic symptoms or ST-segment changes were noted. There were multiple PVCs present during exercise with triplets and three 5-beat runs of

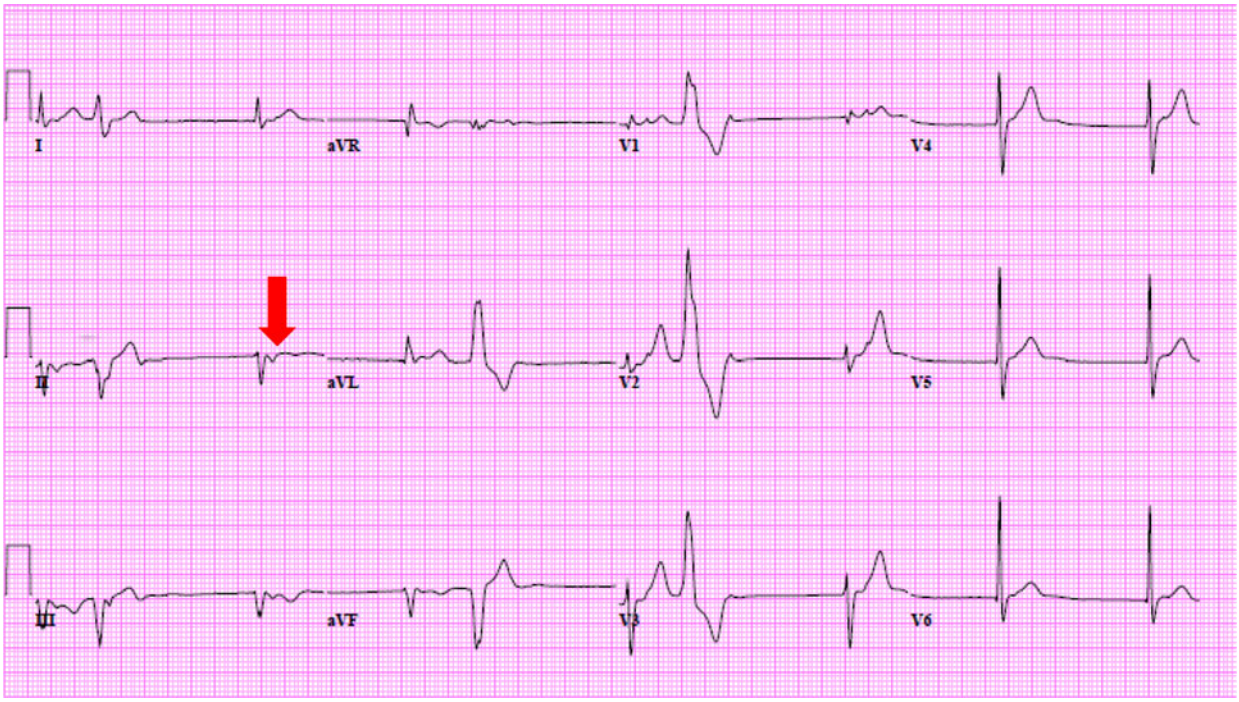

Fig. 1 Resting 12-lead electrocardiogram. There is junctional rhythm at 57 bpm with retrograde conduction at the P-wave (*arrow*), and frequent premature ventricular contractions with a right bundle branch pattern. The QRS duration is mildly prolonged at 106 ms (ms), QT/QTc 426/414 ms, and QRS Axis −67° consistent with a left anterior fascicular block

nonsustained ventricular tachycardia (VT) during the recovery period.

A diagnostic right and left heart catheterization with coronary angiography was performed. The filling pressures (mmHg) were as follows: right atrium 10/9, right ventricle 28/4, pulmonary artery 26/10, pulmonary capillary wedge pressure 14 with ventricular waves to 18, LV end diastolic pressure 12, aorta 126/76 with no gradient on pull-back across the aortic valve. The wave forms were not suggestive of a restrictive pattern. Coronary angiography revealed no significant CAD (Fig. 2).

DISCUSSION

Among patients with a nondilated cardiomyopathy in whom CAD has been excluded, the differential diagnosis includes infiltrative cardiomyopathies such as sarcoidosis and amyloidosis. Inflammatory cardiomyopathy, such as myocarditis, should also be considered. It is important to distinguish between these etiologies since the window of intervention and treatment options remains variable.

Imaging

Noninvasive imaging techniques play a critical role in screening and diagnosing these diseases [1]. Echocardiography is a widely available noninvasive imaging technique; however, it has limited specificity in diagnosing infiltrative and inflammatory cardiomyopathies [5]. Although morphologic and functional features of the heart in restrictive cardiomyopathy can

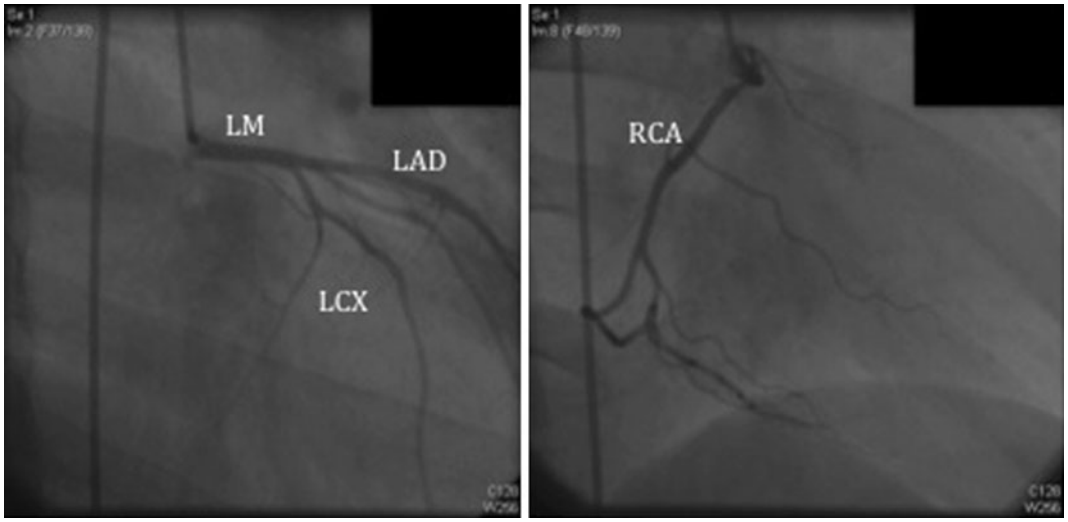

Fig. 2 Coronary angiography. There is right dominant circulation with normal left main coronary artery, left anterior descending artery, and left circumflex artery with no significant lesions

be well characterized by echocardiography, it has relatively poor spatial and contrast resolution [5]. Although newer techniques such as doppler, strain, and speckle echocardiography are useful in detecting abnormal myocardial activity, these imaging modalities cannot delineate tissue characteristics and therefore cannot differentiate between various types of cardiomyopathies [5].

For inflammatory diseases and cardiomyopathy, more specific cross-sectional tissue imaging is required [1]. CMRI has proven to be instrumental in the diagnosis of myocardial and pericardial diseases due to its noninvasiveness, lack of radiation, tomographic imaging, reproducibility, and high spatial resolution [6].

PET-CT can identify an inflammatory process even before structural changes are apparent on CT scanning [7]. PET performed with FDG identifies metabolically active tissue and complements the cross-sectional imaging modalities that provide anatomical features [7]. When patients present with nonspecific symptoms that are difficult to evaluate with routine imaging modalities, whole body imaging with FDG-PET-CT becomes instrumental [7].

Amyloidosis

Systemic amyloidosis results from deposition of misfolded, insoluble protein throughout the body [8]. Cardiac amyloidosis is common in immunoglobulin amyloid light-chain (AL) and transthyretin (TTR) types of amyloidosis. It is caused by deposition of glycoproteins in myocardial interstitium [8]. This leads to concentric thickening of the myocardium and impaired contractility and diastolic dysfunction with restrictive features which in turn can lead to arrhythmias and sudden death [6, 8, 9]. Diagnosis is made by positive endomyocardial biopsy or biopsy of any other organ combined with typical features on cardiac imaging [1]. The mainstay of treatment of amyloidosis is supportive, with use of high-dose diuretics for heart failure that results from restrictive pathophysiology [10]. Given the high rates of

arrhythmias, there is low threshold for introducing implantable cardiac defibrillators and prophylactic antiarrhythmics; however, there are limited data that demonstrate efficacy of these interventions [10]. In AL amyloidosis, chemotherapy has been shown to enhance survival [10]. For TTR amyloidosis, liver transplantation is the standard treatment to remove the main source of plasma TTR [10].

Two-dimensional echocardiography (2D echo) can be used to assess structural anatomy and LV function in cardiac amyloid [11]. Usually all four chambers are involved and thickening of the inter-atrial septum and right atrial free wall is highly specific for amyloidosis [12]. Features suggestive of amyloidosis on 2D echo are thickened myocardium (from amyloid deposition in the interstitial space) with increased myocardial echogenicity and granular speckling [12]. One study compared patients with documented cardiac amyloidosis with controls noting that presence of LV hypertrophy corresponds with sensitivity of 87% and specificity of 81% when increased echogenicity is observed [12]. The specificity rose to 100% if increased atrial thickness was also present [12]. Other features that may also be present include thickened RV myocardium, decreased ventricular cavity size, bi-atrial enlargement, and the presence of pericardial effusion [11], findings more often present in advanced disease.

The most commonly used radionuclide imaging technique in cardiac amyloidosis is bone imaging tracer (Tc-99 m pyrophosphate [PYP] or Tc-99m 3,3-diphosphono-1,2-propanodicarboxylic acid [DPD]) [13, 14] and single photon emission computed tomography (SPECT) tracer I^{123}-metaiodobenzylguanidine (MIBG) [9]. MIBG is an analogue of a neurotransmitter which accumulates in nerve endings and assesses sympathetic nerve activity [9]. MIBG uptake is recorded early at 15 min and later at 4 h (delayed) to assess distribution of sympathetic innervation and degree of impairment of sympathetic nerve impairment [9]. A decrease in MIBG accumulation correlates with severity of amyloid accumulation in patients with familial amyloid polyneuropathy [15]. Although PET tracers show promise by providing better myocardial-sympathetic nervous system innervation, resolution and quantification, thus far no PET tracers specific for amyloidosis have been identified. FDG is not ideal for imaging amyloidosis since it is a metabolic tracer and does not bind to amyloid protein [9].

CMRI is effective in detecting early stages of amyloidosis [10]. The typical features of cardiac amyloidosis such as increased LV wall thickness, bi-atrial enlargement, and pericardial effusions, are well imaged with CMRI [8]. Late gadolinium enhancement and gadolinium kinetics are also useful in assessing severity of amyloid burden and predicting mortality [8]. Delayed enhancement can also be seen in imaging due to increased retention of contrast by expansion of the interstitial space in the amyloid rich area [8]. This results in a classic diffuse, global subendocardial delayed enhancement pattern in a nonvascular distribution [8]. This diffuse heterogeneous enhancement along with biventricular subendocardial enhancement leads to a striped appearance seen in cardiac amyloidosis [6]. Expansion of the extracellular volume can be well imaged with CMRI and has been recently proposed as an early feature of cardiac amyloidosis [16, 17].

Myocarditis

Myocarditis is an acute or chronic inflammation of myocardium caused by a variety of processes including infections, systemic diseases, drugs,

or toxins [1, 18]. Most patients are asymptomatic; however, chest pain, arrhythmias, and rapid onset heart failure have been documented [1]. Furthermore, myocarditis is a major cause of sudden death in adults <40 years of age [18]. Because the symptoms of myocarditis are nonspecific, myocardial biopsy is the only means of making the diagnosis [19]. Focal, mild myocarditis may resolve spontaneously, but mortality of fulminant myocarditis is at least 40% in the first 4 weeks and survival rate of patients with untreated giant cell and eosinophilic myocarditis is 20% in 4 years [19]. If undiagnosed, granulomatous necrotizing myocarditis is fatal [19]. In severe cases, implantation of a ventricular assist device or even heart transplantation may be necessary [20]. Arriving at an early diagnosis is critical since treatment options vary depending on the causative etiology of myocarditis [20]. In acute, chronic and fulminant viral myocarditis, immunosuppression with steroids and intravenous immunoglobulin has been shown to improve outcome [20]. In the rare and often rapidly fatal cases of giant cell myocarditis, where diagnosis is frequently missed until autopsy, initiation of early treatment is critical [21]. Immunosuppressive therapy with triple combination of cyclosporine, azathioprine, and corticosteroids first established in 1990s by Multicenter GCM study group has remained the choice of treatment to achieve remission defined as survival free of heart transplantation [21, 22].

Viral myocarditis is an important cause of myocarditis in North America and Europe [18]. Histologically, this involves focal myocardial apoptosis, necrosis, macrophage activation and tissue edema [1]. Myocarditis involves three phases, namely acute phase characterized by virus entry, subacute phase involving B and T lymphocyte activation and lastly the chronic phase of myocardial remodeling and development of dilated cardiomyopathy [23]. Although endomyocardial biopsy revealing infiltrative lymphocytes and myocytolysis is considered the gold standard, it is limited in sensitivity and specificity [18].

Since there are no specific features of myocarditis on echocardiography, 2D echo is mainly used to rule out other causes of heart failure such as valvular, congenital or pericardial cardiovascular disease [24]. LV systolic dysfunction is commonly seen in myocarditis; however, RV systolic dysfunction is the most important predictor of death [24]. Furthermore, echocardiography can be used to identify acute versus fulminant myocarditis. Acute myocarditis presents with LV dilation, decreased LV function, and normal LV thickness, whereas in fulminant myocarditis LV is not dilated, but is thickened and hypocontractile [25].

The inflammatory pathophysiology underlying myocarditis may be depicted as increased metabolic activity on PET-CT [7]. Myocardial FDG uptake may vary depending on the cause of myocarditis [7]. For example, radiation and chemotherapy are believed to cause microvascular damage leading to impaired perfusion and fatty acid metabolism necessitating switch to high glucose metabolism [22–26]. This may lead to regional or uniform global myocardial involvement [7]. Myocardial inflammation from viral infection (chronic Epstein-Barr virus) may result in increased heterogeneous FDG uptake [27]. Exposure to anthracyclines causes myocardial necrosis also leading to abnormal FDG uptake in the myocardium [6, 7].

Cardiac MR is the most accurate noninvasive imaging modality to diagnose myocarditis with sensitivity and specificity of 100% first reported

by Gagliardi et al. [28] in a cohort of 75 pediatric patients, and reproduced thereafter in other studies with similar results in adults with myocarditis [25]. In the acute and subacute phases, gadolinium-enhanced double-inversion-recovery fast-spin-echo (DIR-FSE) T2- and T1-weighted images show areas of enhancement in the epicardial regions of the left ventricle, septum, and right ventricle [1, 29]. Increased signal intensity is seen for up to 4 weeks after inflammation has begun [1]. Delayed gadolinium enhancement imaging is useful in acute phase of myocarditis before irreversible damage has occurred or in the chronic phase where fibrotic changes have taken place [1]. Hyperenhancing nodules and transmural involvement are common with subepicardial, centromyocardial or mixed myocardial enhancement [30].

Sarcoidosis

Sarcoidosis is a systemic granulomatous disease of unknown etiology [31]. Although only 5% of cases involve the heart, patients may present with acute cardiac failure, arrhythmias or sudden death [31]. Cardiac sarcoidosis has three histologic phases: edema, granulomatous infiltration, and fibrosis and eventual scarring [32]. Usually involvement is predominantly myocardial affecting the LV free wall, basal septum, right ventricle, and finally the atrial wall [1, 31]. This predisposition is believed to be due to increased myocardial mass in these areas [31].

Standard diagnostic criteria for cardiac sarcoidosis developed by the Japanese Ministry of Health and Welfare lack sensitivity and specificity in the absence of diagnostic myocardial biopsy (Table 2) [33, 34]. Even though the gold standard of diagnosis is myocardial biopsy, it has limited utility due to its invasive nature and high false-negative rate secondary to patchy cardiac infiltration [35].

In its early stages, cardiac sarcoidosis is usually clinically silent, rapidly progressing to heart failure, arrhythmias, and even sudden cardiac death [36]. Currently, there are no

Table 2 Modified Japanese Ministry of Health and Welfare guidelines for diagnosing cardiac sarcoidosis

1. Histologic diagnosis group: endomyocardial biopsy demonstrates epithelioid granulomata without caseating granulomata
2. Clinical diagnosis group: in patients with histologic diagnosis of extracardiac sarcoidosis, cardiac sarcoidosis is suspected when 'a' and at least one of criteria 'b' to 'd' is present, and other etiologies such as hypertension and coronary artery disease have been excluded:
   a. Complete right branch bundle block (BBB), left BBB, left-axis deviation, atrioventricular block, ventricular tachycardia, premature ventricular contractions or pathological Q- or ST-T change on resting, or ambulatory electrocardiogram
   b. Abnormal wall motion, regional wall thinning, or dilation of the left ventricle
   c. Perfusion defect by ^{201}thallium-myocardial scintigraphy or abnormal accumulation by 67 Ga-citrate or 99mTc-PYP myocardial scintigraphy
   d. Abnormal intracardiac pressure, low cardiac output, or abnormal wall motion or depressed ejection fraction of the left ventricle

Reproduced with permission from Smedema JP, Snoep G, van Kroonenburgh MP, et al. Evaluation of the accuracy of gadolinium-enhanced cardiovascular magnetic resonance in the diagnosis of cardiac sarcoidosis. *J Am Coll Cardiol*. 2005;45:1683–90

established guidelines for early diagnostic approach [36]. However, in a recent review article by Mantini et al. [36], a step-wise algorithm for patients with suspected cardiac sarcoidosis was proposed. According to the algorithm, patients with proven extra-cardiac sarcoid or patients with suspected sarcoid should be screened with detailed history, physical examination, ECG, and chest X-ray [36]. If the patient is symptomatic, the ECG is abnormal (VT, Mobitz type II or complete heart block on 12-lead, >100 PVCs on 24-hour Holter monitor, or T-wave alternans) or X-ray demonstrates cardiomegaly, follow-up testing is recommended [36]. In a patient with extra-cardiac sarcoid, with no CAD by angiography, further imaging with CMRI, 18F-FDG-PET, rest/stress technetium-99m (^{99m}Tc) sestamibi, or 201-thallium (TI) plus 67-gallium is recommended [36]. If any of the imaging results are abnormal, treatment with steroids should be initiated. Although no randomized controlled studies have demonstrated efficacy of steroid treatment, small cohort studies have shown benefits of oral prednisone at doses 30–60 mg/day for 8–12 weeks with gradual tapering 10–20 mg/day for 6–12 months [36, 37]. Dosing should also be adjusted to counteract known side effects associated with prolonged steroid which include infection, osteoporosis, myopathy, weight gain, and mood changes [36–38]. Furthermore, if the ECG shows type II second-degree or complete atrioventricular block, sustained VT or EF < 50% on echocardiography implantable cardioverter-defibrillator (ICD) placement is recommended [36, 38].

Two-dimensional echocardiographic findings of cardiac sarcoidosis include septal thickening or thinning, general wall motion abnormalities, local aneurysms, LV dilation and systolic dysfunction, or pulmonary artery hypertension [39, 40]. However, myocardial abnormalities earlier on in the disease progression cannot be appreciated on 2D echo.

On PET-CT, active necrotizing granulomatous disease shows up as increased 18F-FDG uptake in myocardium with nonperivascular distribution [1, 41]. This is a particularly useful imaging modality to identify early stages of disease where inflammatory activity is high but myocardial damage is not yet evident. Also, combined imaging of myocardial perfusion (using TI or ^{99m}Tc SPECT, rubidium-82 or N-13 ammonia PET) and FDG imaging can help differentiate myocardial scar from active myocardial sarcoidosis, and identify various stages of the disease process (Fig. 3) [42]. In a study of 22 patients with systemic sarcoidosis, PET-CT had a reported sensitivity and specificity of 100% and 95.5% for diagnosing cardiac sarcoidosis [41]. Since many patients with sarcoidosis require cardiac pacemakers or defibrillators to manage arrhythmias (a contraindication to MR imaging prior to the recent introduction of MRI compatible devices), PET-CT becomes the preferred imaging modality to monitor the disease over time in these patients [7]. CMRI has been shown to be a cost-effective diagnostic technique in evaluating cardiac involvement in sarcoidosis and response to therapy [34]. In a series of 58 patients with biopsy-proven pulmonary sarcoidosis who were being assessed for cardiac sarcoidosis, the sensitivity and specificity of CMRI were 100% and 78%, respectively [34]. On DIR-FSE T2-weighted imaging, the initial edematous phase is seen as localized enhancement of signal intensity and area of hyperintensity within myocardium [1, 35]. Active inflammation appears as delayed enhancement on inversion recovery prepared gradient-echo T1-weighted images [34] and as a focus on cine imaging and bright on DIR-FSE T2-weighted imaging [1]. Scarred segments

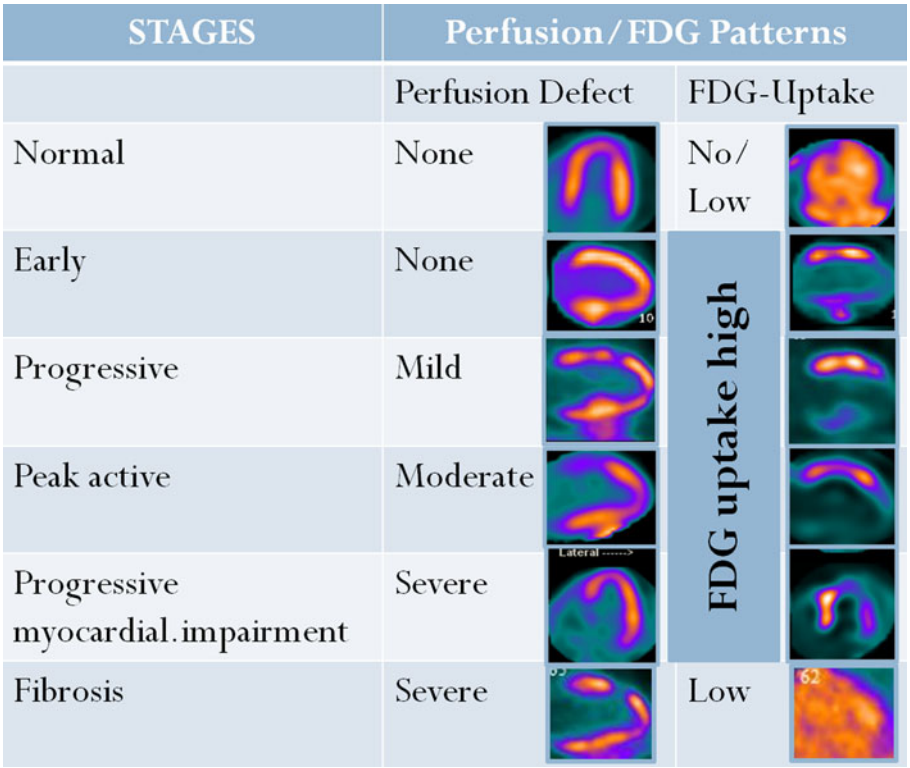

Fig. 3 Perfusion and fluorine-18-fluoro-deoxy-glucose uptake in cardiac sarcoidosis. Perfusion and metabolism patterns in various stages of cardiac sarcoidosis. Reproduced with permission from Skali H, Schulman AR, Dorbala S. (18)F-FDG PET/CT for the assessment of myocardial sarcoidosis. *Curr Cardiol Rep*. 2013;15:352

show up as gadolinium enhanced segments with regional loss of wall thickness and hypokinesis [1, 34].

The major findings of amyloidosis, myocarditis and sarcoidosis with echocardiography, FDG-PET-CT, and cardiac MRI are summarized in Table 3 [1, 7–14, 16, 17, 22–26, 29, 30, 34, 39–41].

CASE WORKUP

Given the patient's gender, age, and symptoms, the patient had intermediate pretest probability for CAD and cardiac catheterization was an acceptable diagnostic approach [43]. With the normal coronary angiography, our suspicion for infiltrative cardiomyopathy was high. RV endomyocardial biopsy demonstrated mild focal myocyte hypertrophy and mild focal interstitial fibrosis with no evidence of active myocarditis, granulomatous inflammation, acute or recent myocardial infarction, amyloid heart disease, or iron deposition. However, since endomyocardial biopsy has a high false-negative rate in cardiac sarcoidosis (due to the focal disease process), we used cardiac MRI and PET-CT to further characterize the pathology due to their high sensitivity for detecting infiltrative and inflammatory cardiomyopathies (Table 4) [12, 22, 29, 35, 41]. Given the reduced LV EF, patient's symptoms and discordant evaluation from cardiac catheterization, patient met appropriate criteria for use of delayed enhancement and CMRI [44]. CMRI showed akinesis of the basal inferolateral walls with corresponding delayed

Table 3 Major findings on imaging studies

	Echocardiography	MRI	FDG-PET	Techniques
Protocol		Four-chamber long-axis, two chamber long-axis, and short axis breath-hold SSFP cine images of heart. In combination with inversion-recovery gradient-echo T1-weighted imaging after injection of gadolinium-based contrast. Delayed enhancement images are obtained after 20 min. If an inflammatory process is suspected, DIR-FSE T2-weighted black blood sequences are obtained	Requires a specific dietary preparation with a high fat and low carbohydrate diet to minimize FDG uptake by normal myocytes Uses PYP or DPD and SPECT tracer MIBG. MIBG uptake is recorded early at 15 min and later at 4 h (delayed) to assess distribution of sympathetic innervation and degree of sympathetic nerve impairment	
Sarcoidosis	Septal thickening/thinning, general wall motion abnormalities, local aneurysms, LV dilation and systolic dysfunction, or pulmonary artery hypertension	On DIR-FSE T2-weighted imaging: Initial edematous phase—localized enhancement of signal intensity and area of hyperintensity within myocardium Active inflammation—delayed enhancement on inversion recovery prepared gradient-echo T1-weighted images and as a focus on cine imaging and bright on DIR-FSE T2-weighted imaging Scarred segments—gadolinium enhanced segments with regional loss of wall thickness and hypokinesis	Increased 18F-FDG uptake in myocardium with nonperivascular distribution	CV-IB has been shown to be superior to 2-dimensional echo in detecting earlier stages of sarcoidosis. CV-IB measures acoustic properties of myocardium and has been shown to be decreased in patients with sarcoidosis

Table 3 continued

	Echocardiography	MRI	FDG-PET	Techniques
Amyloidosis	Thickening of the inter-atrial septum and right atrial free wall Thickened myocardium with increased myocardial echogenicity and granular speckling Thickened RV myocardium, decreased ventricular cavity size, bi-atrial enlargement and presence of pericardial effusion	Diffuse, global subendocardial delayed enhancement pattern in a nonvascular distribution. This diffuse heterogeneous enhancement along with biventricular subendocardial enhancement leads to a striped appearance	No PET tracers specific for amyloidosis have been identified. FDG is not ideal for imaging amyloidosis since it is a metabolic tracer and does not bind to amyloid protein	Recent new techniques in echocardiography such as tissue doppler, strain rate imaging, speckle tracking-based LV torsion analysis, and 3-dimensional echocardiography show promise in detecting disease at a subclinical stage before overt myocardial thickening
Myocarditis	Rule out other causes of heart failure LV systolic dysfunction Acute myocarditis—LV dilation, decreased LV function, and normal LV thickness Fulminant myocarditis—LV thickened and hypocontractile	Acute and subacute phases: gadolinium-enhanced DIR-FSE T2- and T1-weighted images show areas of enhancement in the epicardial regions of the LV, septum, and RV Hyperenhancing nodules and transmural involvement with subepicardial, centromyocardial, or mixed myocardial enhancement	Diffuse regional or uniform global myocardial FDG uptake depending on cause of myocarditis	

Adapted from [1, 7–14, 16, 17, 22–26, 29, 30, 34, 39–41]

CV-IB Cycle-dependent variation of myocardial integrated backscatter, *DIR-FSE* double-inversion-recovery fast spin-echo, *DPD* Tc-99m 3,3-diphosphono-1,2-propanodicarboxylic acid, *FDG* fluorine-18-fluoro-deoxy-glucose, *LV* left ventricle, *MIBG* I^{123}-metaiodobenzylguanidine, *PET* positron emission tomography, *PYP* Tc-99m pyrophosphate, *RV* right ventricle, *SPECT* single photon emission computed tomography tracer, *SSFP* steady-state free precession

Table 4 Sensitivity and specificity of imaging studies

	Echocardiography	MRI	FDG-PET
Sarcoidosis			
Sensitivity (%)	Low	100	100
Specificity (%)		78	95
Amyloidosis			
Sensitivity (%)	87	N/A	N/A
Specificity (%)	81		
Myocarditis			
Sensitivity (%)	Low	100	N/A
Specificity (%)		100	

Adapted from [12, 22, 29, 34, 41]
FDG-PET Fluorine-18-fluoro-deoxy-glucose positron emission tomography, *MRI* magnetic resonance imaging

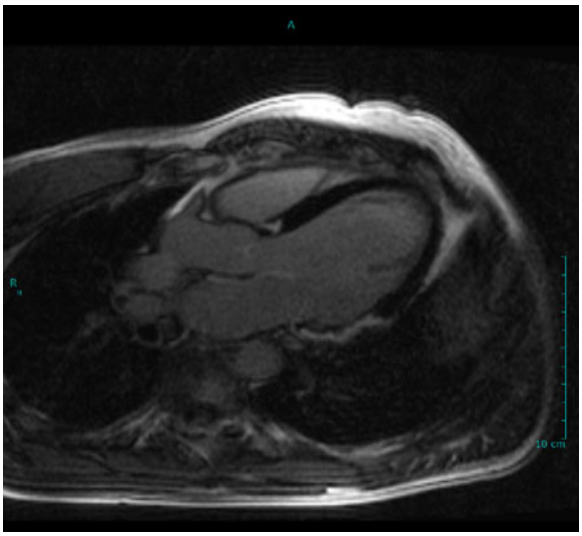

Fig. 4 Cardiac magnetic resonance imaging with focal late gadolinium enhancement suggesting focal inflammation. There is strong accumulation of late gadolinium enhancement involving the basal and mid inferior wall and basal and mid-lateral wall as well as another focus in the basal septum. The pattern of enhancement involves the mid-myocardium and epicardium

hyperenhancement of gadolinium (Fig. 4, Movie 1). With these abnormal imaging results, patient met appropriate criteria for the routine use of radionuclide imaging [43]. FDG-PET-CT showed focal areas of active inflammation in the basal inferolateral walls and focal increased uptake in the mediastinal lymph nodes. Chest CT scan obtained for attenuation correction of the FDG-PET-CT images showed evidence of lymphadenopathy (Fig. 5, Movie 2). Lymph node biopsy was consistent with 'burnt-out' hyalinized granulomas and confirmed the diagnosis of sarcoidosis (Fig. 6). The patient was diagnosed with cardiac sarcoidosis and was treated with prednisone (60 mg orally daily for 7 months). Given the history of ventricular arrhythmia during exercise stress test in this patient with mild-to-moderate LV systolic dysfunction, a dual-chamber pacemaker (DDD) with defibrillator, programmed to treat arrhythmias faster than 170 bpm and DDD with a lower rate limit of 70 bpm, was placed to provide pacing support and prophylaxis against ventricular arrhythmias. The patient was followed initially at 3 months, then every 6 months clinically and with follow-up FDG-PET-CT imaging. Cardiac imaging of the patient showed a continuing stable function. The patient experienced one episode of appropriate defibrillator discharge while watching a sports match.

At follow-up 1 year later, the patient was doing well—with no chest pain, shortness of breath, and no skin, ocular or joint manifestations of sarcoidosis. The patient had normal lung function and now met criteria of New York Heart Association class I (NYHA class I) heart function with no fatigue, palpitations, or dyspnea and otherwise no limitation of physical activity [45]. Given the significant reduction in risk of ICD shock therapy with class III antiarrhythmics versus beta-blockers [46], the recommendation by the electrophysiologist was to initiate sotalol. Repeat imaging with FDG-PET-CT rubidium-82 showed unchanged area of medium-sized focal

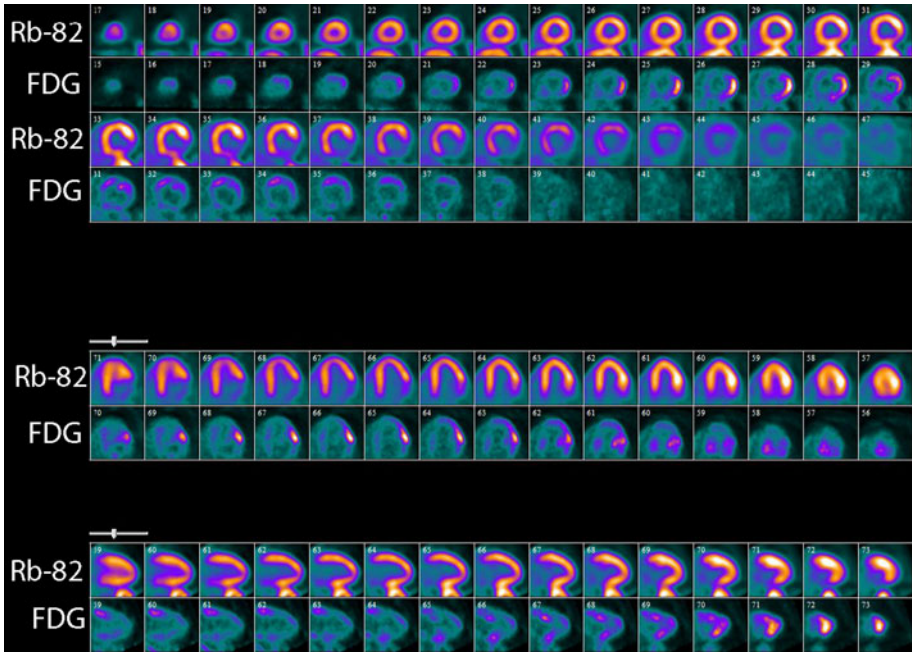

Fig. 5 Myocardial perfusion using rubidium-82 and myocardial fluorine-18-fluoro-deoxy-glucose (FDG) uptake. Uptake is shown in the corresponding segments in alternate rows shown as short axis, horizontal long axis and vertical long axis images. There is a small-to-medium sized perfusion defect involving, the basal inferior wall, basal and mid inferolateral walls. The basal inferior and inferolateral walls show mild mismatch (rest perfusion defect with minimal FDG uptake). There is also increased FDG uptake without a perfusion defect in the regions of the mid-lateral wall, the basal anteroseptal, anterior, and anterolateral walls

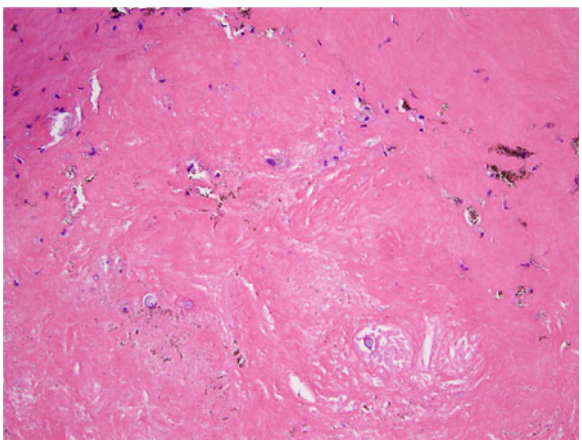

Fig. 6 Histopathology. Lymph node specimen consistent with 'burn-out' hyalinized fibrous granulomas with dystrophic calcifications

FDG uptake in the basal inferolateral wall suggestive of stable active cardiac sarcoid and a persistent prevascular lymph node measuring 0.7–1.2 cm now demonstrating mild FDG activity consistent with likely mildly active sarcoid.

CONCLUSION

The case of a 43-year-old male with nonspecific symptoms of palpitations and left ventricular systolic dysfunction is presented here; the initial workup with echocardiography, exercise stress test, and coronary angiography were nondiagnostic. Given a high suspicion for infiltrative cardiomyopathy, CMRI was used to characterize cardiac wall motion abnormalities, FDG-PET-CT and subsequent cardiac and lymph node biopsies were performed to confirm the diagnosis of cardiac sarcoidosis.

Brief etiologies of two other common cardiomyopathies, namely amyloidosis and

myocarditis, were also reviewed. The advantages and disadvantages of echocardiography, computed tomography radionuclide imaging, and magnetic resonance imaging in working up these cardiomyopathies were discussed and current algorithms, which are helpful to establish a definitive diagnosis, were also described.

ACKNOWLEDGMENTS

The authors would like to thank Dr. Leona A. Doyle for her contribution of the pathophysiology image.

Dr R. Giugliano is the guarantor for this article, and takes responsibility for the integrity of the work as a whole.

Conflict of interest. A. Plitt and Drs S. Dorbala, M.A. Albert and R.P. Giugliano declare that they have no conflict of interest.

Compliance with ethics guidelines. Authors conformed with the Helsinki Declaration of 1975, as revised in 2000 concerning Human and Animal Rights, and that Springer's policy concerning informed consent has been followed.

This article does not contain any studies with human or animal subjects performed by any of the authors.

REFERENCES

1. Sparrow PJ, Merchant N, Provost YL, Doyle DJ, Nguyen ET, Paul NS. CT and MR imaging findings in patients with acquired heart disease at risk for sudden cardiac death. Radiographics. 2009;29:805–23.
2. Loranzo R, Naghavi M, Foreman K, et al. Global and regional mortality from 235 causes of death for 20 age groups in 1990 and 2010: a systematic analysis for the Global Burden of Disease Study 2010. Lancet. 2012;380:2095–128.
3. Srinivasan G, Joseph M, Selvanayagam JB. Recent advances in the imaging assessment of infiltrative cardiomyopathies. Heart. 2013;99:204–13.
4. Bruce RA, Blackmon JR, Jones JW, Strait G. Exercise testing in adult normal subjects and cardiac patients. Pediatrics. 1963;32:742–56.
5. Gupta A, Singh Gulati G, Seth S, Sharma S. Cardiac MRI in restrictive cardiomyopathy. Clin Radiol. 2012;67:95–105.
6. Penugonda N. Cardiac MRI in infiltrative disorders: a concise review. Curr Cardiol Rev. 2010;6:134–6.
7. James OG, Christensen JD, Wong TZ, Borges-Neto S, Koweek LM. Utility of FDG PET/CT in inflammatory cardiovascular disease. Radiographics. 2011;31:1271–86.
8. Maceira AM, Prasad SK, Hawkins PN, Roughton M, Pennell DJ. Cardiovascular magnetic resonance and prognosis in cardiac amyloidosis. J Cardiovasc Magn Reson. 2008;10:54.
9. Glaudemans AW, Slart RH, Zeebregts CJ, et al. Nuclear imaging in cardiac amyloidosis. Eur J Nucl Med Mol Imaging. 2009;36:702–14.
10. Selvanayagam JB, Hawkins PN, Paul B, Myerson SG, Neubauer S. Evaluation and management of the cardiac amyloidosis. J Am Coll Cardiol. 2007;50:2101–10 Erratum in: J Am Coll Cardiol. 2011;57:1501.
11. Tsang W, Lang RM. Echocardiographic evaluation of cardiac amyloid. Curr Cardiol Rep. 2010;12:272–6.
12. Falk RH, Plehn JF, Deering T, et al. Sensitivity and specificity of the echocardiographic features of cardiac amyloidosis. Am J Cardiol. 1987;59:418–22.
13. Perugini E, Guidalotti PL, Salvi F, et al. Noninvasive etiologic diagnosis of cardiac amyloidosis using 99mtc-3,3-diphosphono-1,2-propanodicarboxylic acid scintigraphy. J Am Coll Cardiol. 2005;46:1076–84.
14. Rapezzi C, Guidalotti P, Salvi F, Riva L, Perugini E. Usefulness of 99mtc-dpd scintigraphy in cardiac amyloidosis. J Am Coll Cardiol. 2008;51:1509–10.

15. Tanaka M, Hongo M, Kinoshita O, et al. Iodine-123 metaiodobenzylguanidine scintigraphic assessment of myocardial sympathetic innervation in patients with familial amyloid polyneuropathy. J Am Coll Cardiol. 1997;29:168–74.

16. Banypersad SM, Sado DM, Flett AS, et al. Quantification of myocardial extracellular volume fraction in systemic al amyloidosis: an equilibrium contrast cardiovascular magnetic resonance study. Circ Cardiovasc Imaging. 2013;6:34–9.

17. Mongeon FP, Jerosch-Herold M, Coelho-Filho OR, Blankstein R, Falk RH, Kwong RY. Quantification of extracellular matrix expansion by CMRI in infiltrative heart disease. JACC Cardiovasc Imaging. 2012;5:897–907.

18. Feldman AM, McNamara D. Myocarditis. N Engl J Med. 2000;343:1388–98 Review.

19. Kühl U, Schultheiss HP. Myocarditis—early biopsy allows for tailored regenerative treatment. Dtsch Arztebl Int. 2012;109:361–8.

20. Maisch B, Pankuweit S. Standard and etiology-directed evidence-based therapies in myocarditis: state of the art and future perspectives. Heart Fail Rev. 2012. [Epub ahead of print].

21. Kandolin R, Lehtonen J, Salmenkivi K, Räisänen-Sokolowski A, Lommi J, Kupari M. Diagnosis, treatment, and outcome of giant-cell myocarditis in the era of combined immunosuppression. Circ Heart Fail. 2013;6:15–22.

22. Cooper LT, Berry GJ, Shabetai R, for the Multicenter Giant Cell Myocarditis Study Group Investigators. Idiopathic giant-cell myocarditis—natural history and treatment. N Engl J Med. 1997;336:1860–6.

23. Kindermann I, Barth C, Mahfoud F, et al. Update on myocarditis. J Am Coll Cardiol. 2012;59:779–92 Review.

24. Blauwet LA, Cooper LT. Myocarditis. Prog Cardiovasc Dis. 2010;52:274–88 Review.

25. Felker GM, Boehmer JP, Hruban RH, et al. Echocardiographic findings in fulminant and acute myocarditis. J Am Coll Cardiol. 2000;36: 227–32.

26. Jingu K, Kaneta T, Nemoto K, et al. The utility of 18F-fluorodeoxyglucose positron emission tomography for early diagnosis of radiation-induced myocardial damage. Int J Radiat Oncol Biol Phys. 2006;66:845–51.

27. Takano H, Nakagawa K, Ishio N, et al. Active myocarditis in a patient with chronic active Epstein-Barr virus infection. Int J Cardiol. 2008;130:e11–3.

28. Gagliardi MG, Polletta B, DiRenzi P. MRI for the diagnosis and follow-up of myocarditis. Circulation. 1999;99:458–9.

29. Skouri HN, Dec GW, Friedrich MG, Cooper LT. Noninvasive imaging in myocarditis. J Am Coll Cardiol. 2006;48:2085–93.

30. Dambrin G, Laissy JP, Serfaty JM, Caussin C, Lancelin B, Paul JF. Diagnostic value of ECG-gated multidetector computed tomography in the early phase of suspected acute myocarditis. A preliminary comparative study with cardiac MRI. Eur Radiol. 2007;17:331–8.

31. Roberts WC, McAllister HA Jr, Ferrans VJ. Sarcoidosis of the heart. A clinicopathologic study of 35 necropsy patients (group 1) and review of 78 previously described necropsy patients (group 11). Am J Med. 1977;63:86–108 Review.

32. Sekhri V, Sanal S, Delorenzo LJ, Aronow WS, Maguire GP. Cardiac sarcoidosis: a comprehensive review. Arch Med Sci. 2011;7:546–54.

33. Hiraga H, Yuwai K, Hiroe M, et al. Guideline for the Diagnosis of Cardiac Sarcoidosis Study Report on Diffuse Pulmonary Diseases. Tokyo: Japanese Ministry of Health and Welfare; 1993. p. 23–4.

34. Smedema JP, Snoep G, van Kroonenburgh MP, et al. Evaluation of the accuracy of gadolinium-enhanced cardiovascular magnetic resonance in the diagnosis of cardiac sarcoidosis. J Am Coll Cardiol. 2005;45:1683–90.

35. Osman F, Foundon A, Leyva P, Pitt M, Murray RG. Early diagnosis of cardiac sarcoidosis using magnetic resonance imaging. Int J Cardiol. 2008;125:e4–5.

36. Mantini N, Williams B Jr, Stewart J, Rubinsztain L, Kacharava A. Cardiac sarcoid: a clinician's review on how to approach the patient with cardiac sarcoid. Clin Cardiol. 2012;35:410–5.

37. Chiu CZ, Nakatani S, Zhang G, et al. Prevention of left ventricular remodeling by long-term corticosteroid therapy in patients with cardiac sarcoidosis. Am J Cardiol. 2005;95:143–6.

38. Winterbauer RH, Kirtland SH, Corley DE. Treatment with corticosteroids. Clin Chest Med. 1997;18:843–51.

39. Hyodo E, Hozumi T, Takemoto Y, et al. Early detection of cardiac involvement in patients with sarcoidosis by a non-invasive method with

ultrasonic tissue characterisation. Heart. 2004;90: 1275–80.

40. Sköld CM, Larsen FF, Rasmussen E, Pehrsson SK, Eklund AG. Determination of cardiac involvement in sarcoidosis by magnetic resonance imaging and Doppler echocardiography. J Intern Med. 2002;252: 465–71.

41. Okumura W, Iwasaki T, Toyama T, et al. Usefulness of fasting 18F-FDG PET in identification of cardiac sarcoidosis. J Nucl Med. 2004;45:1989–98.

42. Skali H, Schulman AR, Dorbala S. (18)F-FDG PET/CT for the assessment of myocardial sarcoidosis. Curr Cardiol Rep. 2013;15:352.

43. Hendel RC, Berman DS, Di Carli MF, et al. ACCF/ASNC/ACR/AHA/ASE/SCCT/SCMRI/SNM 2009 Appropriate Use Criteria for Cardiac Radionuclide Imaging: A Report of the American College of Cardiology Foundation Appropriate Use Criteria Task Force, the American Society of Nuclear Cardiology, the American College of Radiology, the American Heart Association, the American Society of Echocardiography, the Society of Cardiovascular Computed Tomography, the Society for Cardiovascular Magnetic Resonance, and the Society of Nuclear Medicine Endorsed by the American College of Emergency Physicians. J Am Coll Cardiol. 2009;53:2201–29.

44. Hendel RC, Patel MR, Kramer CM, et al. ACCF/ACR/SCCT/SCMRI/ASNC/NASCI/SCAI/SIR 2006 Appropriateness Criteria for Cardiac Computed Tomography and Cardiac Magnetic Resonance Imaging: A Report of the American College of Cardiology Foundation Quality Strategic Directions Committee Appropriateness Criteria Working Group, American College of Radiology, Society of Cardiovascular Computed Tomography, Society for Cardiovascular Magnetic Resonance, American Society of Nuclear Cardiology, North American Society for Cardiac Imaging, Society for Cardiovascular Angiography and Interventions, and Society of Interventional Radiology. J Am Coll Cardiol. 2006;48:1475–97.

45. Raphael C, Briscoe C, Davies J, et al. Limitations of the New York Heart Association functional classification system and self-reported walking distances in chronic heart failure. Heart. 2007;93: 476–82.

46. Ferreira-González I, Dos-Subirá L, Guyatt GH. Adjunctive antiarrhythmic drug therapy in patients with implantable cardioverter defibrillators: a systematic review. Eur Heart J. 2007;28:469–77.